

## Temperature Effects in Varactors and Multipliers

J. East and I. Mehdi

Solid State Electronics Laboratory

The University of Michigan

JPE

### Abstract

Varactor diode multipliers are a critical part of many THz measurement systems. The power and efficiencies of these devices limit the available power for THz sources. Varactor operation is determined by the physics of the varactor device and a careful doping profile design is needed to optimize the performance. Higher doped devices are limited by junction breakdown and lower doped structures are limited by current saturation. Higher doped structures typically have higher efficiencies and lower doped structures typically have higher powers at the same operating frequency and impedance level. However, the device material properties are also a function of the operating temperature. Recent experimental evidence has shown that the power output of a multiplier can be improved by cooling the device. We have used a particle Monte Carlo simulation to investigate the temperature dependent velocity vs. electric field in GaAs. This information was then included in a nonlinear device circuit simulator to predict multiplier performance for various temperatures and device designs. This paper will describe the results of this analysis of temperature dependent multiplier operation.

### I Introduction

The goal of this paper is to investigate the temperature dependent performance of GaAs based Schottky diode frequency multipliers. The performance of these multipliers is an important limitation on the overall performance of submillimeter and THz imaging systems. Recent experimental evidence indicates that these multipliers can have improved performance with cooling. This paper will discuss a simplified device model to investigate this temperature dependence. The next section of the paper will present a temperature and doping dependent transport model for GaAs obtained from a Monte Carlo based transport model. The results of this model were parameterized

to provide information for a device model. Section III describes the nonlinear device circuit model used to include velocity saturation effects and the conditions used in the multiplier simulation. Section IV presents results for doping, temperature and frequency dependent multiplier performance. The paper is summarized in Section V.

## II Monte Carlo Modeling of GaAs Transport

The transport properties of GaAs play an important part in the operation of high frequency GaAs Schottky barrier frequency multipliers. The velocity characteristics in the undepleted region of the diode determine the saturation characteristics and thus the power and the efficiency. To date, most varactor designs have been based on room temperature heat sink operation. However, recent measurements have shown that cooling improves the operation, so we need a better understanding of temperature dependent transport. We have used a Monte Carlo simulation of GaAs electron velocities vs. electric field, doping and temperature to quantify the transport. The simulation is a simple 2 valley parabolic band approximation [1], [2]. The code includes most of the characteristics of a more complex approach, yet is fast enough for the type of parameter extraction needed for this study. The simulation was run for temperatures between 150 and 450 K, corresponding to a range between a cooled heat sink and typical higher temperature operation. The data was fit to a velocity vs. electric field curve of the form [3].

$$v(E) = \frac{\mu E + v_{\text{sat}} \left(\frac{E}{E_p}\right)^4}{1 + \left(\frac{E}{E_p}\right)^4}, \quad (1)$$

where  $\mu, v_{\text{sat}}$  and  $E_p$  are fitting parameters that depend on the temperature and doping. In the low field limit  $v(E) = \mu E$  and at high fields  $v(E) = v_{\text{sat}}$ . Typical results are shown in Fig. 1 for a doping of  $10^{17}/\text{cm}^3$ . The peak velocities based on Eqn. 1 can then be collected and plotted. A plot of the peak velocity vs. temperature and doping is shown in Fig. 2. The peak velocities and the mobilities can be fit to equations of the form

$$V_{\text{peak}}(T) = V_{\text{peak}}(300)(T/300)^x. \quad (2)$$

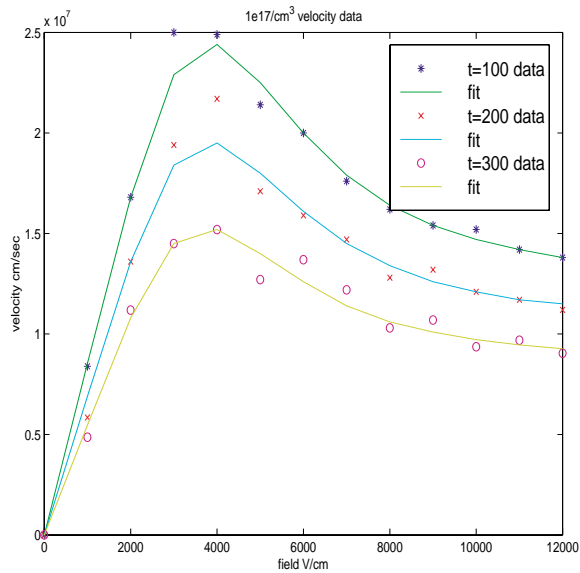


Figure 1: GaAs temperature and field dependent velocities  $N_d = 10^{17}/\text{cm}^3$

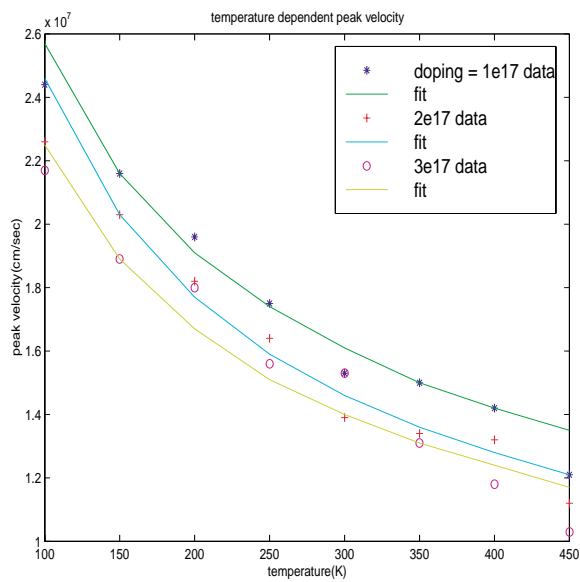


Figure 2: GaAs temperature and doping dependent peak velocities

and

$$\mu(T) = \mu_{300}(T/300)^x. \quad (3)$$

These expressions can then be used in a nonlinear multiplier simulation to investigate temperature dependent operation. We also need to model the breakdown voltage. The breakdown voltage will depend on the doping profile and the temperature. If we assume an abrupt junction and neglect the temperature dependence, the breakdown voltage can be approximated by

$$V_{\text{breakdown}}(N_d) = 60(N_d/10^{16}\text{cm}^{-3})^y. \quad (4)$$

This expression is shown in Fig. 3. We can use this material information to investigate device operation.

### III Multiplier Modeling

The next step is to simulate multiplier performance for a variety of operating temperatures, frequencies and powers levels. We need a device model that takes velocity saturation effects into account. These effects were first described by Kollberg et.al. [4] A simple physical model for this effect based on separating the structure into an abrupt depletion layer and an undoped epitaxial layer with transport in the bulk determined by a velocity vs. electric field curve was described by East et.al. [5] This model has been used in a nonlinear circuit simulator to investigate devices under different operating conditions.

We need a way to compare devices for a range of operating conditions. However, the multiplier performance will strongly depend on the bias point, the frequency and the embedding impedances. We need a consistent comparison. In this paper we fix the input Q of the circuit. This in effect sets the type of operation, with lower Q devices acting more like nonlinear resistors and higher Q devices acting more like nonlinear capacitors. With a fixed source impedance, the device can be tuned to match the circuit, rather than the more conventional approach of designing a circuit around a given diode. Adjusting the device area scales the impedance level and adjusting the bias changes the ratio of the input real and reactive impedance. The combination inside an optimization loop can adjust the nonlinear input impedance

to match the source impedance. The harmonic load will also effect the input impedance and efficiency of the multiplier. The device harmonic output impedance will conjugate match the harmonic load. We need to search the output impedance plane to find the embedding impedance that produces the highest efficiency for a given input power. This search becomes the inner loop in the simulation. The outer loop is the available local oscillator power. The input parameters of the simulation are the epitaxial layer doping and length, the frequency, the device breakdown voltage, the peak velocity, the mobility and a local oscillator power step. The simulation loops through the code increasing the available power until the maximum voltage across the semiconductor depletion layer becomes larger than the breakdown voltage. The outputs of the simulation are the pump frequency input impedance as a check on the convergence of the simulation, the output power and efficiency, the optimal output embedding impedance, the device area and bias and useful internal parameters such as the peak electric field in the bulk and the peak depletion layer voltage. The simulation can use the temperature dependent velocity characteristics described in the last section to investigate the temperature characteristics of multipliers.

#### IV Temperature, Doping and Frequency Dependent Performance

Before we investigate temperature dependent multiplier operation, we first consider constant temperature characteristics. The first example is a multiplier operating with an input frequency of 50 GHz with a peak velocity of  $1.6 \times 10^7$  cm/sec corresponding to an operating temperature of 300 K and an input impedance of  $50 + j100$ . Fig. 4 shows the efficiency vs. available input power and Fig. 5 shows the output power for a range of epitaxial layer dopings. These two figures show many of the design tradeoffs in multipliers. For this 50 GHz room temperature operation, the  $3 \times 10^{16}$ /cm<sup>2</sup> device is operating in velocity saturation . The multiplier efficiency decreases over the entire operating range. Increasing the doping to  $4 \times 10^{16}$ /cm<sup>2</sup> reduces the saturation effects. The  $6 \times 10^{16}$ /cm<sup>2</sup> device is showing little saturation and is operating with a nearly constant efficiency over it's entire operating range. The corresponding power plot shows the effect of the breakdown voltage on the power output. The lower doped structure have a larger breakdown voltage and can support a larger input power before breakdown, nearly 300 mW. However, the larger input power doesn't produce a larger output power due

to efficiency reduction caused by velocity saturation. The  $4 \times 10^{16}/\text{cm}^2$  device is operating near the onset of saturation. Its efficiency is decreasing at higher drive levels, causing the output power to nearly saturate at higher drive levels. The higher doping level reduces the breakdown voltage and the corresponding input power, but this structure produces the most power of the 3 cases in this figure. Finally, the  $6 \times 10^{16}/\text{cm}^2$  device, with the best efficiency of the group, is limited by its smaller breakdown voltage to an input power of 100 mW. Its peak output power is similar to the lowest doped case. Further increasing the doping will reduce the breakdown voltage and allow the device to operate without saturation effects. This will have only a small effect on the efficiency but will further reduce the output power due to the reduced breakdown voltage and input power.

Next let's consider the effect of varying the temperature. Consider a multiplier doped at  $3 \times 10^{16}/\text{cm}^3$  operating with an input frequency of 50 GHz and a source impedance of  $50 + j100$ . The operating temperature varies between 100 and 400 K with a variation in the saturated velocity, given by Eqn. 2, ranging between 1.4 and  $2.5 \times 10^7$  cm/sec. This design showed strong saturation effects in Figs. 4 and 5. The resulting temperature dependent efficiency is shown in Fig. 6. This device shows a strong temperature dependent performance. At 300 and 400K the multiplier is strongly saturated, with efficiencies that are monotonically dropping with pump power. Decreasing the temperature from 300 to 200K, with a corresponding increase in the saturated velocity from  $1.6$  to  $1.9 \times 10^7$  cm/sec improves the efficiency at the peak pump power point from 10 to 20%. An additional decrease in the temperature to 100K increases the velocity enough to eliminate most of the saturation effects. The efficiency is nearly constant with pump power. These efficiency variations will have a strong effect on the available power from the multiplier. The temperature dependent output power is shown in Fig. 7. The 100K device can produce more than 4 times the power of the room temperature structure.

This improvement in power and efficiency at lower temperatures occurs because the higher saturated velocities at lower temperatures can support more current. An example of a structure that does not have much improvement at reduced temperatures is shown in Fig. 8. This is the optimal room temperature device from Fig. 4. This device has a large enough doping to support the current at room temperature. Lowering the temperature will increase the

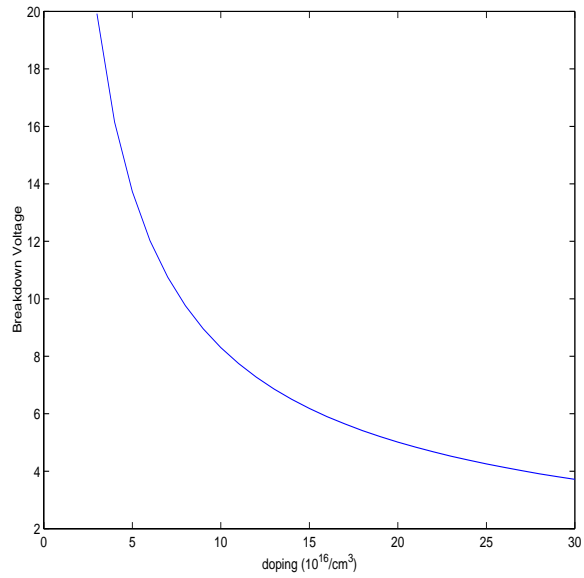


Figure 3: GaAs Junction Breakdown Voltage vs. Doping

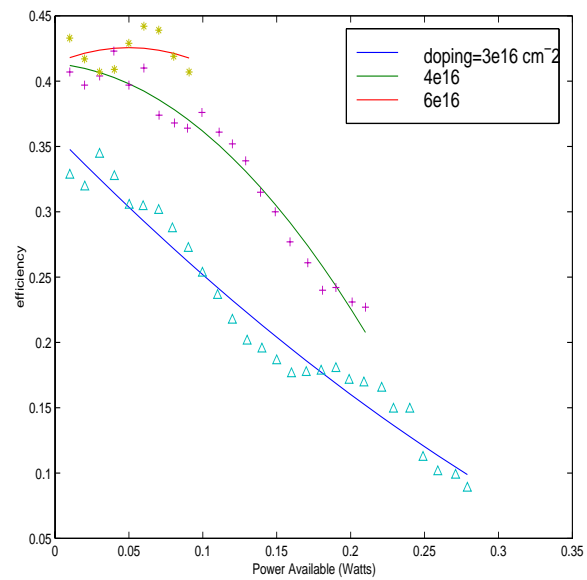


Figure 4: Doping Dependent Efficiency for  $F=50$  GHz,  $T=300$ ,  $Z_{in}=50+j100$

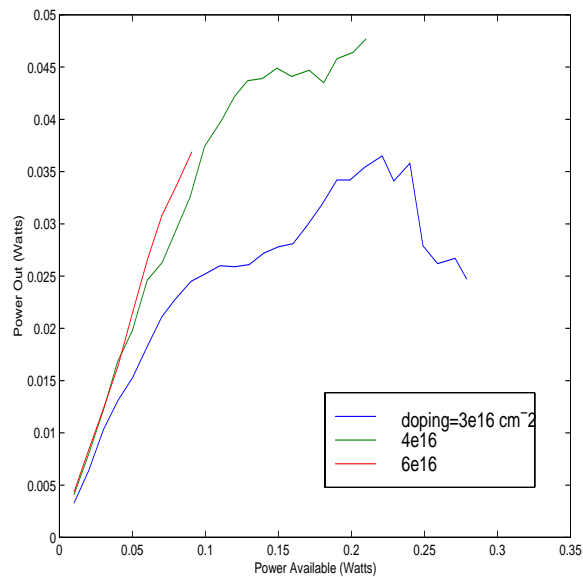


Figure 5: Doping Dependent Power for  $F=50$  GHz,  $T=300$ ,  $Z_{in}=50+j100$

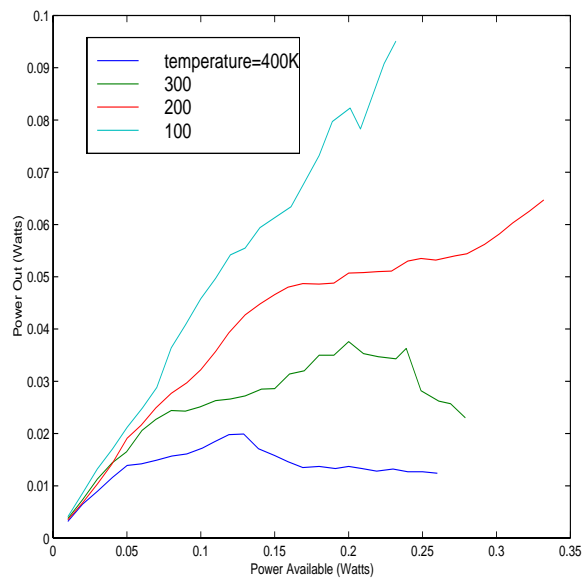


Figure 6: Temperature Dependent Efficiency for  $F=50$  GHz,  $N_d = 3 \times 10^{16}/\text{cm}^3$ ,  $Z_{in}=50+j100$



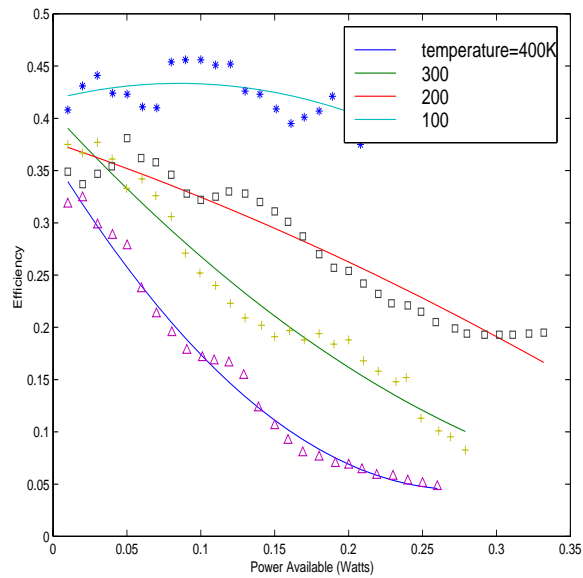


Figure 7: Temperature Dependent Power for  $F=50$  GHz,  $N_d = 3 \times 10^{16}/\text{cm}^3$ ,  $Z_{in}=50+j100$

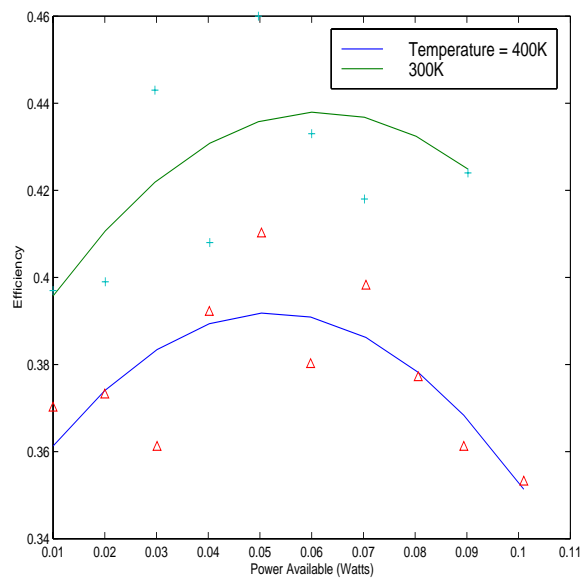


Figure 8: Temperature Dependent Power for  $F=50$  GHz,  $N_d = 6 \times 10^{16}/\text{cm}^3$ ,  $Z_{in}=50+j100$

saturated velocity, but the additional velocity is not utilized by the device, so there is only a modest improvement in the efficiency at the lower temperature. This device is limited by its breakdown voltage, and the higher current available at lower temperatures gives only a small performance improvement.

Similar temperature and doping dependent calculations were carried out for input frequencies of 100 and 200 GHz. The resulting power vs. frequency at room temperature and 100 K is plotted in Fig. ???. The figure shows that a properly designed low temperature device can produce approximately twice the power of a room temperature one.

## V Summary

This paper has discussed the results of a frequency dependent investigation of multiplier performance. The results show that the temperature dependent peak velocity plays an important role in performance. The optimal design depends on the tradeoff between current saturation and breakdown and the design for peak power can be different than the peak efficiency design. The power and efficiency also depend on the temperature. Reducing the temperature increases the peak velocity and can change the mode of operation. Devices designed for room temperature operation can have modest improvement with reduced temperature. A device that is current saturated for room temperature operation can greatly improve its performance with cooling. The difference in output power for a well designed room temperature device and a corresponding low temperature design can be as much as a factor of 2.

## References

- [1] Fawcett, W., Boardman, A.D. and Swain, S., "Monte Carlo Determination of Electron Transport Properties in Gallium Arsenide," *J. Phys. Chem. Solids* vol. 31, no. 9, pp. 1963-1990, September, 1970.
- [2] Ruch, J.G. and Fawcett, W., "Temperature Dependent of the Transport Properties of Gallium Arsenide Determined by a Monte Carlo Method," *Journal of applied Physics*, vol. 41, no. 9, pp. 3843-3849, August, 1970.

- [3] Bauhahn,P.E.,“Properties of Semiconductor Materials and Microwave Transit Time Devices,” Ph.D. Thesis, The University of Michigan, 1977.
- [4] Kollberg,E., Tolmunen,M., Frerking,M. and East,J., ”Current Saturation in Submillimeter Wave Varactors,” IEEE Trans. on Microwave Theory and Techniques, vol. 40, no. 5, May,1992, pp. 831-838.
- [5] East,J., Kollberg,E. and Frerking,M., ”Performance Limitations of Varactor Multipliers,” Fourth International Conference on Space Terahertz Technology, March, 1993, pp. 98-114.

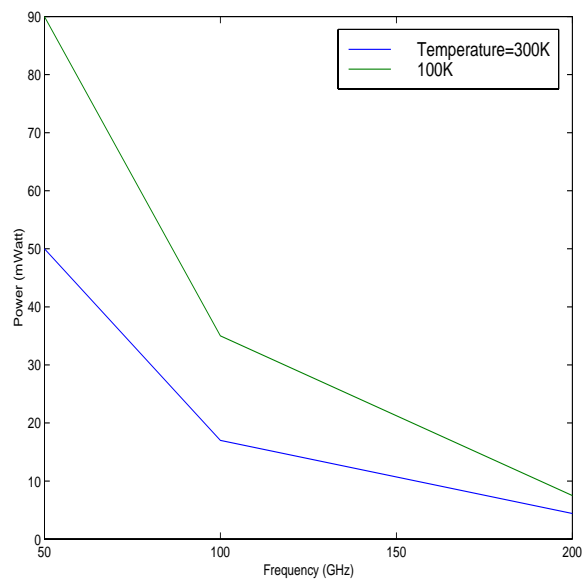


Figure 9: Summary of Frequency Dependent Power vs. Frequency and Temperature

Part of the research described in this paper was carried out at the Jet Propulsion Laboratory, California Institute of Technology, under a contract with the National Aeronautics and Space Administration.